

## **A Numerical Method for Variable Surface Tension Effects in Non-Isothermal Atomization with Overset Grids**

P. Brady<sup>1\*</sup>; M. Herrmann<sup>1</sup>, and J. M. Lopez<sup>2</sup>

<sup>1</sup>School of Mechanical, Aerospace, Chemical, and Materials Engineering

<sup>2</sup>School of Mathematical and Statistical Sciences  
Arizona State University, Tempe, AZ 85287

### **Abstract**

Overset or overlapping grids have been used to simulate a wide variety of flows. A typical overset grid consists of at least 2 curvilinear grids which cover a domain and overlap where they intersect. Flow field variables are transferred between the grids in the overlap region via appropriate interpolation functions. Overset grids can thus vastly simplify the grid generation process for complex 3-D geometries and flows with moving boundaries. They also lend themselves to problems requiring high resolution in a region of the domain. Here we aim to couple an overset-grid method to our flow solver and interface tracking scheme for the purpose of high resolution atomization simulations. Simulating atomization accurately is a huge numerical challenge since time and length scales vary over several orders of magnitude, the phase interface is a material discontinuity, and surface tension forces are singular. The Refined Level Set Grid (RLSG) method, coupled to the moving overset meshing solver (OSM) presented here, is one numerical approach to simulate the primary breakup process of liquid jets and sheets in detail. With the RLSG method, the liquid/gas phase interface is tracked by a level set method using an auxiliary high resolution equidistant Cartesian grid. This not only allows for application of higher-order WENO schemes retaining their full order of accuracy both for advecting and reinitializing the level set scalar, but it also provides the necessary high resolution of the phase interface geometry during topology change events in an efficient manner. In many technical applications of interest atomization occurs in non-isothermal environments, like for example in combustion devices. In these devices, thermal fluctuations can be significant on length scales associated with the liquid atomization process. Since the surface tension force is a function of local temperature, these thermal fluctuations can result in large local variations of the surface tension force, thereby potentially significantly impacting the details of the atomization process. The OSM solver is introduced to handle these potentially large thermal fluctuations in the vicinity of the interface. This allows us to resolve the complex thermal boundary layers that can develop without the expense of refining the flow solver grid. A numerical method will be presented which couples our flow solver, level set grid, and overset grid for the purpose of incorporating thermal Marangoni forces into the balanced force algorithm in order to study their impact on the atomization process. The method of manufactured solutions is used to verify the temperature solver in OSM. The interpolation routines for the velocity and temperature fields are also verified.

---

\*Corresponding Author: peter.brady@asu.edu

## Introduction

Composite, overset or overlapping grids, first introduced by [1], have been applied to a wide variety of flows. Flow inside an internal combustion engine with moving rigid boundaries was simulated using overlapping grids by [2]. Using overset grids, the flow inside an artificial heart was simulated by [3]. A fractional-step method for solving the Navier-Stokes equations on overset grids was developed by [4] and tested by examining vortex shedding around a cylinder at  $Re = 100$ . The authors also report the ability to use a hybrid of implicit/explicit schemes on the various component grids to alleviate time-step restrictions. In [5] a *mass flux based interpolation* scheme is developed to ensure global mass conservation between composite grids and applied to channel flow with obstructions to demonstrate the possibility of using overset meshes in flows with large pressure and velocity gradients. An implicit pressure-correction scheme using non-conservative interpolation while still enforcing a solenoidal velocity field between composite grids was shown in [6]. The authors also demonstrate the use of composite meshes of different refinement levels appropriate to the local flow field behavior. In [7], the authors develop an overset grid method which is interface aligned and moves with the interface. Due to the nature of the problem they investigate, only the flow outside the interface is solved for while the interface is advanced using a kinematic condition. In this paper we propose a non-rigid moving overset grid method (OSM) coupled the RLSG [8] interface tracking scheme. The OSM will move with the interface and enable us to better resolve the field in the vicinity of the interface during non-isothermal atomization.

In non-isothermal atomization applications thermal fluctuations can have a significant impact on the dynamics of liquid/gas interfaces because, for most gas/liquid combinations, both surface tension and phase transition depend strongly on the local temperature. An important technical application where both surface tension forces and phase transition are dominant is the atomization of liquid fuels for combustion processes. For combustion to occur, the liquid fuel needs to be atomized, evaporated, and mixed with an oxidizer. The ensuing chemical reactions can generate temperature variations on the order of  $10^3\text{K}$  over small length scales of the order of  $10^{-3}\text{m}$ . Due to the strong dependence of surface tension on temperature, the temperature fluctuations result in Marangoni forces that impact the flowfield at the gas/liquid interface, which in turn alter the interfacial temperature distribution via the induced interfacial flow [9]. Although the ratio of global iner-

tial to surface tension forces is typically large in these applications, atomization, which is the first in the sequence of processes leading to combustion, always occurs on small scales (involving droplets which are many orders of magnitude smaller than the diameter of the initial liquid jet). At these scales, surface tension forces are dominant. Variations in temperature, resulting in variations in surface tension forces, can thus influence atomization significantly.

However, to the knowledge of the authors, there exists no detailed experimental data set analyzing the phase interface dynamics during atomization in this situation. Numerical simulations, on the other hand, can study the impact of thermally induced variations in surface tension forces and can thus help determine whether they play a role in the atomization outcome. The large temperature fluctuations which develop near the interface will be solved using a refined OSM. Should this prove effective, OSM may be equipped in the future to solve the full Navier-Stokes equations.

## Governing equations

Consider a spherical drop of one fluid with radius  $r_0$  placed in a bulk fluid. The two fluids are immiscible with, in general, different densities, viscosities and thermal properties. Throughout, subscript  $d$  refers to properties of the drop phase and subscript  $b$  to those of the bulk phase. We shall use the initial radius of the drop,  $r_0$ , as the length scale, with some appropriate velocity,  $U$  as the velocity scale. The non-dimensional Navier-Stokes equations governing the motion of an unsteady, incompressible, immiscible, two-fluid system, are

$$\begin{aligned} \rho_r \left( \frac{\partial \mathbf{u}}{\partial t} + \mathbf{u} \cdot \nabla \mathbf{u} \right) = \\ -\nabla P + \frac{1}{Re} \nabla \cdot \mu_r (\nabla \mathbf{u} + \nabla^T \mathbf{u}) + \frac{1}{We} \mathbf{F}, \\ \nabla \cdot \mathbf{u} = 0 \end{aligned} \quad (1)$$

where  $\mathbf{u}$  is the non-dimensional velocity,  $P$  the non-dimensional pressure, the relative dynamic viscosity is  $\mu_r = 1$  in the bulk phase and  $\mu_r = \mu_d/\mu_b$  in the drop phase, and the relative density is  $\rho_r = 1$  in the bulk phase and  $\rho_r = \rho_d/\rho_b$  in the drop phase. The Reynolds, Weber and Capillary numbers are

$$Re = \frac{Ur_0}{\nu_b}, \quad We = \frac{\rho_b r_0 U^2}{\sigma_0}, \quad Ca = \frac{\mu_b U}{\sigma_0}, \quad (2)$$

where  $\nu_b$  is the bulk phase kinematic viscosity and  $\sigma_0$  is the surface tension evaluated at some reference temperature  $T_0$ .

The surface force  $\mathbf{F}$ , which is non-zero only at

the location of the drop interface  $\mathbf{x}_f$ , is [10]

$$\frac{1}{We} \mathbf{F}(\mathbf{x}) = \frac{1}{Re} \left( \frac{1}{Ca} \kappa \delta \mathbf{n} + (T - T_0) \kappa \delta \mathbf{n} + \nabla_{\parallel} T \delta \right), \quad (3)$$

where  $\kappa$  and  $\mathbf{n}$  are the local interface curvature and normal vector,  $\nabla_{\parallel}$  is the tangential surface derivative, and  $\delta$  is the interface delta function. The first two terms on the right-hand side correspond to the isothermal normal stress balance and the temperature-dependent normal stress balance, and the third term corresponds to the Marangoni force. The non-dimensional heat equation for the temperature is

$$\rho_r c_{pr} \left( \frac{\partial T}{\partial t} + \nabla \cdot (T \mathbf{u}) \right) = \frac{1}{Ma} \nabla \cdot (k_r \nabla T), \quad (4)$$

where the relative thermal conductivity  $k_r = 1$  in the bulk phase and  $k_r = k_d/k_b$  in the drop, the relative specific heat  $c_{pr} = 1$  in the bulk phase and  $c_{pr} = c_{pd}/c_{pb}$  in the drop, and the Marangoni and Prandtl numbers are

$$Ma = \frac{Ur_0}{\alpha_b}, \quad Pr = \nu_b/\alpha_b. \quad (5)$$

## Numerics

To determine the location  $\mathbf{x}_f$  of the phase interface we employ a level set approach by defining the level set scalar at the interface

$$G(\mathbf{x}_f, t) = 0, \quad (6)$$

with  $G(\mathbf{x}, t) > 0$  in the drop and  $G(\mathbf{x}, t) < 0$  in the bulk phase. Differentiating Eq. (6) with respect to time yields the level set equation,

$$\frac{\partial G}{\partial t} + \mathbf{u} \cdot \nabla G = 0. \quad (7)$$

All level set related equations are solved using the Refined Level Set Grid (RLSG) method in a separate level set solver LIT [8] using an auxiliary high-resolution  $G$ -grid with the fifth-order WENO scheme of [11] in conjunction with the third-order TVD Runge-Kutta time discretization of [12]. The phase interface curvature  $\kappa$  is evaluated on the  $G$ -grid using a second-order interface projection method [8].

The Navier-Stokes equations together with the temperature and continuity equation are solved by the finite volume, structured flow solver NGA [13]. The coupling of LIT and NGA has been detailed in [8] and will not be reviewed here.

Near the vicinity of the interface the temperature equation is currently solved on OSM using the fifth-order WENO scheme of [11] in conjunction with the

third-order TVD Runge-Kutta time discretization of [12]. The fluid properties are calculated using volume fraction,  $\psi$ , weighted averages,

$$\alpha(\mathbf{x}) = \psi \alpha_b + (1 - \psi) \alpha_d. \quad (8)$$

OSM is linked to NGA and LIT through the interpolation operators  $Q_O$ ,  $Q_L$ , and  $Q_N$ . The temperature is passed from OSM to NGA for use as a boundary condition via  $Q_O$ . Data from NGA is passed to OSM using  $Q_N$ . The level-set scalar  $G$  is interpolated from LIT to OSM via  $Q_L$ . When passing data between grids, it is of paramount importance to use interpolation of the appropriate order [14]. The heat equation on NGA is solved using a  $3^d$  order QUICK scheme, so tricubic interpolation was adopted for the transfer of variables. In [15], the authors develop a general scheme for conservative interpolation since straightforward interpolation is not, in general, conservative. The impact of conservative vs. non-conservative interpolation will be addressed in the future.

For a given timestep,  $n \rightarrow n + 1$ , NGA uses  $Q_O(T_{OSM}^n)$  as a dirichlet boundary condition, where  $T_{OSM}^n$  is the temperature field on OSM. Likewise, OSM uses  $Q_N(T_{NGA}^n)$  as a dirichlet boundary condition for the,  $n \rightarrow n + 1$ , timestep. Figure 1 is a diagram showing the OSM and NGA grids at the start of timestep  $n$  illustrating the overlap of the two grids and the interpolated boundary conditions.

## Coupling and Structure of OSM

OSM is designed to provide a highly resolved temperature field in the vicinity of the interface as it deforms and moves through the bulk phase. The high resolution is relatively inexpensive because OSM is only active in a narrow band around the interface. Currently, OSM uses a band structure similar to LIT which is presented in great detail in [8]. OSM is split into five bands,  $\mathcal{OA}$ ,  $\mathcal{OT}$ ,  $\mathcal{OTB}$ ,  $\mathcal{OO}$  and  $\mathcal{OOB}$  as shown in figure 1. The  $\mathcal{OA}$  band contains all cells which have a  $G$  value opposite their neighbor and thus, either contain the interface or are directly adjacent to it. Cells in the  $\mathcal{OTB}$  (Overset Inner Boundary) band are used in the interpolation operation to compute  $Q_O(T_{OSM})$ . The  $\mathcal{OO}$  (Overset Overlap) band ensures that the overlap distance,  $d_o$ , stays constant under grid refinement [14]. The  $\mathcal{OOB}$  band contains the interpolated NGA temperatures,  $Q_N(T_{NGA})$ , which are used as a dirichlet boundary condition during timestepping.

The algorithm for a time step  $n$  is shown below to illustrate the coupling of LIT, NGA and OSM.

- The velocity  $\mathbf{U}_{NGA}^n$  is interpolated from NGA to LIT.

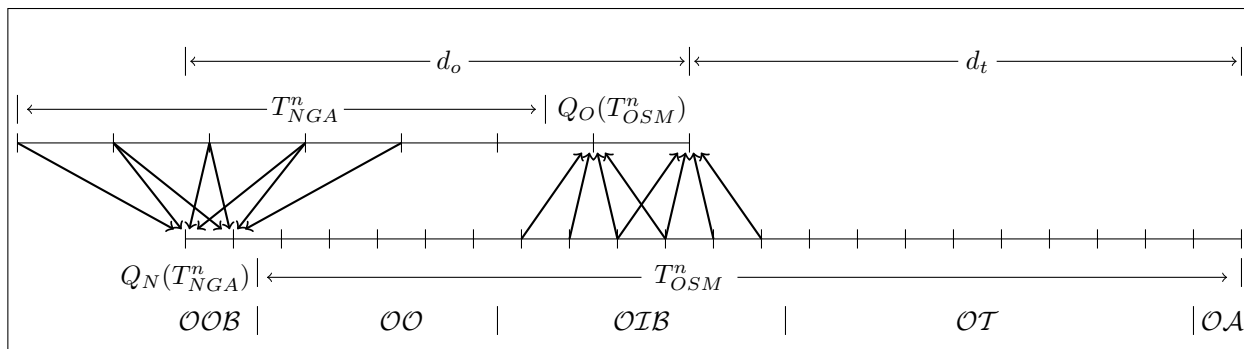


**Figure 1.** 1-D sketch of OSM (bottom) and NGA (top) grids, with overlap distance  $d_o$  and transport distance  $d_t$  shown. Arrows indicate direction of interpolation. Interior temperatures on NGA and OSM grids are  $T_{NGA}^n$  and  $T_{OSM}^n$ , respectively. Boundary temperatures determined from interpolation operators are  $Q_O(T_{OSM}^n)$  and  $Q_N(T_{NGA}^n)$ . The band structure of OSM is also shown.

- The levelset  $G^n$  is advanced to  $G^{n+1}$  in LIT.
- Volume integration is performed on  $G^{n+1}$  to determine the volume fraction in NGA [16]. This is used to compute the material properties about the interface.
- Compute  $G_{OSM}^{n+1} = Q_L(G^{n+1})$  and use it to determine new OSM  $\mathcal{OA}$  band and the volume fraction,  $\psi_{OSM}^{n+1}$ . OSM is regrown around the new  $\mathcal{OA}$  band using the band grow algorithm of [8].
- Compute  $\mathbf{U}_{OSM}^n = Q_N(\mathbf{U}_{NGA}^n)$  throughout the whole OSM domain.
- Compute  $Q_N(T_{NGA}^n)$  for the OSM cells in the  $\mathcal{OOB}$  band.
- Update  $T_{OSM}^n \rightarrow T_{OSM}^{n+1}$  for  $\mathcal{OA}$  through  $\mathcal{OO}$  bands using the  $\mathcal{OOB}$  band as a dirichlet boundary condition.
- Update  $\mathbf{U}_{NGA}^n \rightarrow \mathbf{U}_{NGA}^{n+1}$  over the whole NGA domain. Update  $T_{NGA}^n \rightarrow T_{NGA}^{n+1}$  using  $Q_O(T_{OSM}^n)$  as a dirichlet boundary condition where appropriate.
- Use the  $\mathcal{OIB}$  band to compute  $Q_O(T_{OSM}^{n+1})$  for NGA to use as boundary conditions for the next timestep.

The overset meshing solver OSM, level set solver LIT and the flow solver NGA are coupled using the code coupling paradigm CHIMPS [17].

## Results

To verify this code we will make use of the method of manufactured solutions. Our prescribed

solution for an axisymmetric coordinate system,  $(x, r, \theta)$ , is

$$T(\mathbf{x}) = \exp(2x) \cos(r). \quad (9)$$

Figure 2 shows that fifth order convergence is observed in OSM for the three cases of single-phase constant  $\alpha$ , single-phase variable  $\alpha$ , and two-phase variable  $\alpha$ . The next step will be to use this method on the coupled NGA-LIT-OSM system for the three cases. Once that is successful, the manufactured solution will vary with time to verify the temporal accuracy. After this, the code will be tested against previous solutions with a moving interface.

To test the interpolator  $Q_O$ , a cubic temperature field was defined on the OSM grid and compared to  $Q_O(T_{OSM})$ . The error was on the order of  $10^{-14}$ . The same tests were performed for  $Q_N$  yielding similar results.

## Conclusions

Overset grids have proved to be a valuable tool in many simulations. In this report, we have presented a numerical method to for a moving, deformable overset meshing solver for two-phase flow. This would allow us to resolve the large temperature gradients which can occur in non-isothermal atomization and more accurately study the effects of variable surface tension on the drop atomization process.

At present, several test cases remain to verify the code. Once completed, indepth timing studies will be performed to determine if overset meshing is a viable solution for atomization simulations.

## Acknowledgments

This work was supported by NSF grant number DMS-0808045.

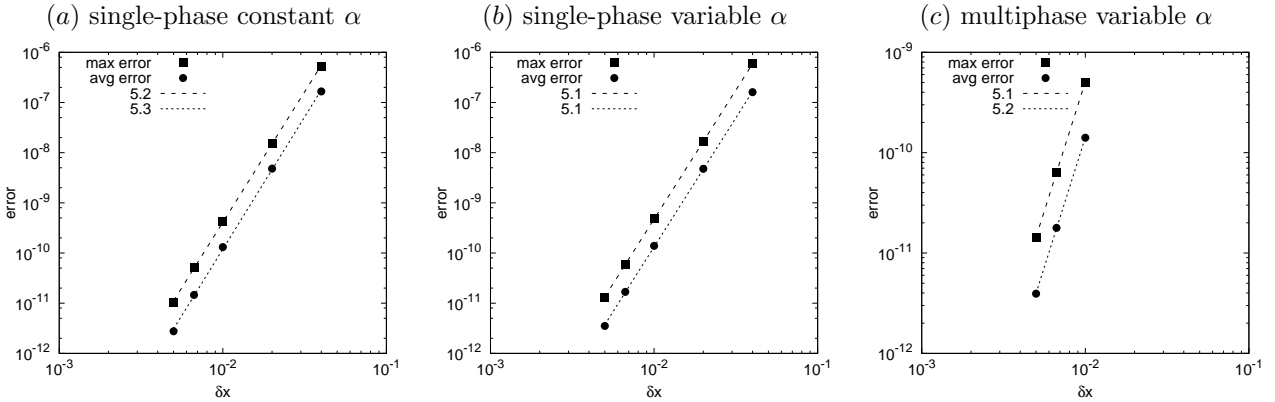


**Figure 2.** Error vs grid spacing for the maximum error and the average error showing fifth order convergence for manufactured solution.

## References

- [1] Benek, J., Steger, J., et al. *AIAA Paper 83-1944*, 1983.
- [2] Tu, J. and Fuchs, L. *Int. J. Numer. Meth. Fluids* 15:693–714, 1992.
- [3] C., Kwak, S., et al. *ASME J. Biomech. Eng* 119(4):452–461, 1997.
- [4] Burton, T. and Eaton, J. *J. Comput. Phys.* 177:336–364, 2002.
- [5] Tang, H., Jones, S., et al. *J. Comput. Phys.* 191:567–600, 2003.
- [6] Ahusborde, E. and Glockner, S. *Int. J. Numer. Meth. Fluids* 62:784–801, 2010.
- [7] Fast, P. and Shelley, M. *J. Comput. Phys.* 195:117–142, 2004.
- [8] Herrmann, M. *J. Comput. Phys.* 227(4):2674–2706, 2008.
- [9] Levich, V.G. and Krylov, V.S. *Ann. Rev. Fluid Mech.* 1:293–316, 1969.
- [10] Landau, L.D. and Lifshitz, E.M. *Fluid Mechanics*. New York: Pergamon, 1959.
- [11] Jiang, G.S. and Peng, D. *SIAM J. Sci. Comput.* 21(6):2126–2143, 2000.
- [12] Shu, C.W. *SIAM J. Sci. Stat. Comput.* 9(6):1073–1084, 1988.
- [13] Desjardins, O., Blanquart, G., et al. *J. Comput. Phys.* 227(15):7125–7159, 2008.
- [14] Chesshire, G. and Henshaw, W. *J. Comput. Phys.* 90:1–64, 1990.
- [15] Chesshire, G. and Henshaw, W. *SIAM J. Sci. Comput.* 15(4):819–845, 1994.
- [16] van der Pijl, S.P., Segal, A., et al. *Int. J. Numer. Meth. Fluids* 47:339–361, 2005.
- [17] Alonso, J.J., Hahn, S., et al. In *42nd AIAA/ASME/SAE/ASEE Joint Propulsion Conference & Exhibit*, number 2006-5274 in AIAA-Paper. 2006.